IEEE Access
Multidisciplinary | Rapid Review | Open Access Journal

Received April 15, 2019, accepted May 3, 2019, date of publication May 20, 2019, date of current version June 4, 2019.

Digital Object Identifier 10.1109/ACCESS.2019.2917821

Integrated Demand Response Mechanism for Industrial Energy System Based on Multi-Energy Interaction

ZIQING JIANG, (Student Member, IEEE), QIAN AI, (Senior Member, IEEE), AND RAN HAO, (Student Member, IEEE)

Key Laboratory of Control of Power Transmission and Conversion, Ministry of Education, Department of Electrical Engineering, Shanghai Jiao Tong University, Shanghai 200240, China

Corresponding author: Ziqing Jiang (jiangzq_jollay@sjtu.edu.cn)

This work was supported in part by the National Natural Science Foundation of China, under Grant U1866206.

ABSTRACT With the development of energy integration technologies, the conventional scope of demand response has been extended to the integrated demand response (IDR), which imparts the flexibility to consumers' energy demand. This paper explores interaction patterns for multi-energy demand management and proposes an IDR mechanism for the industrial integrated energy system. The mechanism exploits three interaction patterns to promote the interaction between the demand and supply of multiple energy systems. The incentive payment is provided not only for curtailing interruptible electric load, but also for adjusting flexible heating and cooling loads. The coupling characteristics of industrial consumers' multi-energy demands are then modeled to reflect the mutual influence between the consumption behaviors for different energy sources. Besides, based on the coupling of CCHP (Combined Cooling, Heating, and Power) energy outputs, the demand-supply interaction model is also proposed, which could change the electric generation by affecting consumers' heating and cooling demands. The optimization model of the IDR is then established with the objective of minimizing the total dispatch cost. The simulation results show that compared with conventional DR programs, the total dispatch cost and consumers' energy procurement cost are both reduced. The CCHP could also benefit from this mechanism. Furthermore, the impact of the coupling characteristics and the incentive price on the dispatch cost is also analyzed.

INDEX TERMS Demand response, integrated energy system, optimal dispatch, multi-energy coordination.

NOMENCLATURE

i	Index of consumers
j	Index of CCHP units
t	Index of time intervals
n	Number of consumers
T	Number of time intervals
P_{in}^e/P_{in}^g	Electricity/gas input of energy hub
$P_{out}^e/P_{out}^h/P_{out}^q$	Electricity/heating/cooling output of energy hub
η_T/η_F	Efficiency of transformer/ gas furnace
η_{MT}^g/η_{MT}^e	Thermal/electric efficiency of micro turbine
μ_{eh}/μ_{eq}	Coupling coefficients of consumers' energy demand
$L_{i,t}^e/L_{i,t}^h/L_{i,t}^q$	Electricity/heating/cooling load
$P_{j,t}^e/P_{j,t}^h/P_{j,t}^q$	CCHP output of electricity/heating/cooling
$C_{i,t}^{IL}$	Incentive payment for IL
$\Delta L_{i,\min}^{ee}/\Delta L_{i,\max}^{ee}$	Lower/upper limit of consumers' IL
λ_h	Heat price
ρ_h/ρ_q	Incentive price for heating/cooling
ε_i	Demand elasticity of consumers
$L_{i,\max}^h$	Maximum heat demand of consumers
σ_{eh}	Heat-to-electricity ratio of CCHP
S_t^{es}	Amount of energy stored in storage system
$P_{in,t}^{es}/P_{out,t}^{es}$	Charging/discharging power of energy storage
η_{in}/η_{out}	Charging/discharging efficiency of energy storage

The associate editor coordinating the review of this manuscript and approving it for publication was Lei Wang.

δ_{es}	Dissipation coefficient of energy storage system
l	Length of the pipe
h	Heat transfer coefficient
T_s/T_r	Supply/Return temperature
T_a	Ambient temperature
T_{in}/T_{out}	Inlet/outlet temperature
C_w	Specific heat of water
m_i	Heat water mass flow

I. INTRODUCTION

The flexibility of consumers' electric demand has significantly enhanced due to the advances in smart grid technology and advanced metering infrastructure [1]. Many demand response (DR) mechanisms have then been designed and applied to achieve certain goals such as peak load shaving or renewable energy accommodation [2].

Recent years, the development of energy cogeneration and integration technologies has facilitated the evolution from DR in smart grid to integrated demand response (IDR) in integrated energy systems (IES) [3], [4]. Like electric demand, the energy demand of consumers could also be flexible and adjustable, if given appropriate incentives. Thus, a reasonable IDR mechanism becomes an important approach to encouraging multi-energy interaction, achieving integrated energy management and optimizing resource configuration.

So far, conventional DR strategies and mechanisms for many purposes have been intensively studied, such as economical operation [5], [6], system frequency regulation [7], [8], congestion management [9]–[10], and some valuable results have been obtained. However, these studies mainly focus on the dispatch of flexible electric demand, such as interruptible load (IL) and direct load control (DLC). While these measures could actually accomplish the goal of load shaping or frequency regulation, they also lead to a certain degree of discomfort, as consumers' demand is partly compromised [11]. Moreover, the response of electric demand cannot achieve the comprehensive energy optimization, especially for consumers with demand for various forms of energy.

With the development of IES-related techniques, the joint dispatch of DR and electro-thermal equipment has been studied for the optimal operation of IES. Liang *et al.* [12] propose a new dispatch framework for virtual power plants (VPPs) considering correlated DR, which coordinates the operation of CCHP (Combined Cooling, Heating and Power) and DR units. In [13], a two-stage coordinated operation method is proposed to coordinate CCHP and flexible electric and thermal loads based on price-based DR. Cui *et al.* [14] propose a bi-level coordination model for electricity and gas network while considering both coupon-based DR and interruptible-load based DR. However, these researches consider CCHP and flexible loads as two separate approaches to achieving optimal dispatch, whereas the former is not regarded as a demand side resource which could be employed for the purpose of IDR. Moreover, the CCHP is usually presumed in these studies to be possessed by the VPP or microgrid operator. In other words, the interaction remains between consumers and the operator, whereas no other participants are envolved.

In fact, CCHP and other energy converting entities play an essential role in multi-energy interaction. There are already some researches trying to study the application of CCHP and heat pumps on DR, and some valuable conclusions are drawn [15]–[20]. To quantify the available flexibility in heat pumps, some indexes are identified in [15] and [16] to analyze its potential and impact on demand side management programs. In [17], a new expected thermal discomfort metric is defined to optimize the thermal storage-based flexible DR. Tasdighi *et al.* [18] present an optimal scheduling model for a micro-CHP based microgrid on the basis of temperature dependent thermal load modeling. These researches mainly study the thermal behavior of resident consumers or commercial buildings based on comfort or temperature constraints, which cannot be applied to industrial consumers whose heat demand is mainly determined by production schedules.

Moreover, most of these researches try to affect the electric demand by changing and scheduling consumers' thermostatically controlled loads, which is the interaction between the demand sides of heat system and power system. However, the interaction between the demand side of one energy system and the supply side of another, e.g. how the change of heat demand could affect the supply of electricity, is not investigated.

There have been a few relevant attempts to deal with this problem. In [21], DR is integrated with the coalitional game where prosumers can adjust their flexible thermal and electric loads simultaneously to minimize the coalition operation cost. Liu *et al.* [22] propose a heat-electricity-coupled DR model by dynamically selecting the heat-match mode and the electricity-match mode of CCHP units. But these papers does not consider the coupling of multi-energy demand, e.g., how the heat load changes with the electric load because of energy substitute effect and machines consuming more than one types of energy. In [11], an IDR program is developed for the electricity and natural gas networks. The interaction among energy hubs is modeled as an ordinal potential game with unique Nash equilibrium. Shao *et al.* [23] incorporate the flexible electric and heating demands into the centralized energy dispatch model and establish a two-level optimization model for the purpose of maximizing social welfare. These studies usually consider consumers' flexible demand as directly controllable resources, and little work has been devoted to addressing the problem how the incentive compensation is designed and provided in IDR programs. Given that consumers' response is essentially a profit-pursuing activity, a mechanism with reasonable incentive patterns is important to the actual implementation of IDR.

This paper explores interaction patterns for multi-energy demand management and proposes an IDR mechanism for industrial integrated energy system. The mechanism exploits three interaction patterns to promote the interaction between the demand and supply of multiple energy systems. In greater detail, this paper contributes in the following ways.

1) An IDR mechanism with three interaction patterns is designed for load curtailment. The incentive payment is provided not only for curtailing interruptible electric load, but also for increasing flexible heating and cooling loads.

2) The coupling relationship of consumers' multi-energy demands is modeled to reflect the mutual influence between the consumption behaviors for different energy sources. Besides, the demand-supply interaction model is also proposed, which could change the electricity generation by affecting consumers' heating and cooling demands. Based on the two models, the optimization model of IDR is proposed with the objective of minimizing total dispatch cost.

3) The proposed IDR mechanism is simulated, and consumers' responsive behaviors are analyzed. Simulation results show that the total dispatch cost and consumers' energy procurement cost are both reduced, compared with conventional DR programs. CCHP could also benefit from this mechanism. Furthermore, the impact of the incentive price on the dispatch cost is also analyzed.

The rest of the paper is organized as following. Section II proposes three interaction patterns which could be applied to achieve IDR. Section III proposes the coupling model of multi-energy demands, the supply-demand interaction model, and the optimization model of IDR. Section IV discusses experimental results and Section V presents conclusions.

II. INTERACTION PATTERNS OF INTEGRATED DEMAND RESPONSE

A. COUPLING RELATIONSHIP WITHIN IES

The IES studied in this paper is a combination of CCHP based district heating system and electric power system, which supplies electricity, heating and cooling for consumers. Involving energy generation units, transmission infrastructure and consumers' multi-energy demands, it could promote energy cascade utilization and significantly improve comprehensive energy efficiency.

The most distinguished difference between the regional electric power system and IES lies in the mutual influence of generation and consumption of multiple energy sources, which brings forth the coupling relationship on both the supply side and the demand side [24].

Typically, the energy generation units can be divided into three categories, i.e., electricity-only units, heat-only units and cogeneration units. The cogeneration equipment normally refers to CCHP whose electricity production and heat production are coupled depending on the operation mode. The heat-only units are usually gas furnaces. Generally, the coupling relationship on the supply side of IES can be described by the energy hub model [25], which is as following:

$$\begin{bmatrix} P_{out}^{e} \\ P_{out}^{h} \end{bmatrix} = \begin{bmatrix} \eta_T & \omega_1 \eta_{MT}^{e} \\ 0 & (1-\omega_1)\eta_F + \omega_1 \eta_{MT}^{g} \end{bmatrix} \begin{bmatrix} P_{in}^{e} \\ P_{in}^{g} \end{bmatrix} \tag{1}$$

where ω_1 denotes the ratio of gas consumed by micro turbine.

Incorporating the cooling power supplied by the absorption refrigeration, the extended energy hub model can be modified into (2). It can be easily deduced that the increase in the generation of heating and cooling power could also lead to the increase in that of electricity, and vice versa.

$$\begin{bmatrix} P_{out}^{e} \\ P_{out}^{h} \\ P_{out}^{q} \end{bmatrix} = \begin{bmatrix} \eta_T & \omega_1 \eta_{MT}^{e} \\ 0 & (1-\omega_2)\left[(1-\omega_1)\eta_F + \omega_1 \eta_{MT}^{g}\right] \\ 0 & \omega_2 \sigma_{hq}[(1-\omega_1)\eta_F + \omega_1 \eta_{MT}^{g}] \end{bmatrix} \begin{bmatrix} P_{in}^{e} \\ P_{out}^{g} \end{bmatrix} \tag{2}$$

where ω_2 denotes the ratio of heat consumed for cooling generation, and σ_{hq} denotes the efficiency of the refrigeration.

The coupling relationship also exists on the demand side. For one thing, some machines used in industrial production consume more than one type of energy, such as rubber mixing machines which consume both electricity and heat. Thus, the operation of these machines will cause both the electric demand and the heat demand to rise. For another, the substitute effect also exists among different energy sources. For example, when the heat produced by CCHP is cheaper, direct heat supply could substitute for the electric boiler, and the electric load will be decreased. In this way, as the demand for one energy source changes, the demand for another will also change. Furthermore, the change of the price of one energy source could also affect the demand for others. Further details on the coupling relationship of multi-energy demand are discussed in later sections.

B. INTERACTION PATTERNS OF IDR

The principle of IDR, which is similar to that of conventional electric DR, is to encourage consumers to adjust their energy demand by providing reasonable compensation. By taking advantage of the coupling relationships mentioned above, the measures to motivate consumers could be intensively diversified.

Based on the analysis above, this paper designs an IDR mechanism with three interaction patterns, which could achieve the curtailment of electric load by direct and/or indirect means. Specifically, the three patterns are as follows:

1) DIRECT LOAD CURTAILMENT

It is the common way of conventional DR programs, which stimulates consumers to cut down part of their load by providing incentive payment.

2) COUPLING OF MULTI-ENERGY DEMANDS

As aforementioned, the electric load of some users' drops as their demands for heating and cooling increase. Such demands are encouraged, which would have the same effect as the interruptible load does.

3) MULTI-ENERGY INTERACTION BETWEEN SUPPLY AND DEMAND

Consumers are encouraged to increase their demands for heating and cooling. To satisfy the increasing need, CCHP has to raise the corresponding supply. According to the coupling characteristics on the supply side expressed in (2), the power generation will also increase and the net load of IES will be reduced.

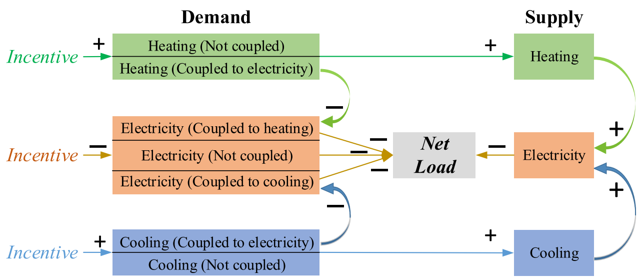

FIGURE 1. Interaction process of IDR.

The principles of the three interaction patterns can be elaborated by Fig.1. The incentive compensation is provided for curtailing electric load in pattern 1, and for increasing heating and cooling loads in pattern 2 and 3. The advantage of this mechanism lies in that, unlike the conventional patterns to encourage consumers to cut down their load, it is more acceptable for them to raise their demand, and the overall energy procurement cost could be reduced. Therefore, the motivation to participate in IDR programs would also rise. Moreover, the costs of applying the three patterns are different, which is affected by consumer type, demand level, and CCHP operation point. By applying interaction patterns of lower expenses, the total compensation payment would also drop.

C. INTERACTION PROCESS OF IDR

In this paper, we assume that there is an operator in each regional industrial IES, who is in charge of the implementation of IDR. It determines the dispatch plan which satisfies the load curtailment index and coordinates the interaction between consumers, CCHP and itself. The index denotes the amount and time of load curtailment. In market mechanism, it is obtained by bidding for ancillary services like reserve, while in regulated mechanism, it is notified by the ISO (Independent System Operator) in the upper level according to the system operation needs.

Large consumers are equipped with integrated energy management system (IEMS), which could analyze and manage the demands for electricity, heating and cooling. CCHP is not possessed by the operator, but operates for its own benefits. Compared with bulk power systems, IES is usually smaller in size and area, thus the network structure is not considered.

The entire interaction process of IDR program is as follows:

1) The operator performs day-ahead load forecast, and reports it to the ISO, or bids into the electricity market.
2) The operator acquires the load curtailment index, either from the ISO or from the clearing results of the market.
3) The operator determines the dispatch plan by solving the optimization model of IDR, which is proposed in Section III, and informs consumers and CCHP of the results.
4) If any consumer or CCHP cannot respond as instructed, the operator will reschedule the dispatch plan. Otherwise, the response will be executed.
5) Next day, consumers adjust their energy demand at the specified time, either decreasing the electric load or increasing the heating and cooling load. CCHP correspondingly adjusts their energy production to balance the load. The net load of IES will be curtailed as planned.

III. DISPATCH MODEL OF INTEGRATED DEMAND RESPONSE

A. MODELING THE COUPLING OF MULTI-ENERGY DEMAND

The electric, heating and cooling loads of consumers are mutually affected, and the general coupling relationship on the demand side can be expressed by (3-5).

$$L_{i,t}^{e} = L_{i,t}^{ee} + L_{i,t}^{eh} + L_{i,t}^{eq} \tag{3}$$
$$L_{i,t}^{h} = L_{i,t}^{hh} + L_{i,t}^{he} + L_{i,t}^{hq} \tag{4}$$
$$L_{i,t}^{q} = L_{i,t}^{qq} + L_{i,t}^{qh} + L_{i,t}^{qe} \tag{5}$$

where $L_{i,t}^{eh}$ signifies the part of electric load which is coupled to the heat load, $L_{i,t}^{eq}$ signifies the part coupled to the cooling load, and $L_{i,t}^{ee}$ signifies the part not coupled. The meanings of other variables are similar.

Unlike the HVAC (Heating, Ventilation, and Air Conditioning) load of residential consumers, the industrial load is consumed mainly for production purpose, and determined mainly by the production plan, so it cannot be modelled by common temperature and comfort level models [26].

Generally, the heat-electricity coupled equipment can be divided into two types. For the first type, the electric load remains constant once the equipment is turned on, no matter how the heat load changes. While for the second type, the electric load changes with the heat load. In this way, $L_{i,t}^{eh}$ and $L_{i,t}^{eq}$ xcan be expressed as (6-7).

$$L_{i,t}^{eh} = \varphi_{eh} + \mu_{eh} L_{i,t}^{he} \tag{6}$$
$$L_{i,t}^{eq} = \varphi_{eq} + \mu_{eq} L_{i,t}^{qe} \tag{7}$$

where φ_{eh} and φ_{eq} are the constant parts; μ_{eh} and μ_{eq} are the coupling coefficients which can be either positive or negative. The former signifies the kind of equipment which entails both electricity and heating/cooling power, while the latter refers to the substitute effect. In practice, μ_{eh} and μ_{eq} may be time-varying. Through (6) and (7), the change of $L_{i,t}^{eh}$ and $L_{i,t}^{eq}$ can be expressed as follows.

$$\Delta L_{i,t}^{eh} = \varphi_{eh} + \mu_{eh}\left(L_{i,t}^{he} + \Delta L_{i,t}^{he}\right) - \varphi_{eh} - \mu_{eh}L_{i,t}^{he} = \mu_{eh}\Delta L_{i,t}^{he} \quad (8)$$

$$\Delta L_{i,t}^{eq} = \varphi_{eq} + \mu_{eq}\left(L_{i,t}^{qe} + \Delta L_{i,t}^{qe}\right) - \varphi_{eq} - \mu_{eq}L_{i,t}^{qe} = \mu_{eq}\Delta L_{i,t}^{qe} \quad (9)$$

Thus, equations (3)–(5) can be modified into

$$\Delta L_{i,t}^{e} = \Delta L_{i,t}^{ee} + \mu_{eh}\Delta L_{i,t}^{he} + \mu_{eq}\Delta L_{i,t}^{qe} \quad (10)$$

$$\Delta L_{i,t}^{h} = \Delta L_{i,t}^{hh} + \Delta L_{i,t}^{he} + \mu_{hq}\Delta L_{i,t}^{qh} \quad (11)$$

$$\Delta L_{i,t}^{q} = \Delta L_{i,t}^{qq} + \Delta L_{i,t}^{qe} + \Delta L_{i,t}^{qh} \quad (12)$$

The heating and cooling consuming facilities are usually associated with productive load, the curtailment of which may affect consumers' revenue. Thus, the interruptible electric load of industrial consumers is usually non-productive load, i.e. $L_{i,t}^{ee}$. In contrast, $\Delta L_{i,t}^{he}$ and $\Delta L_{i,t}^{qe}$ are dispatched by pattern 2, while $\Delta L_{i,t}^{qq}$, $\Delta L_{i,t}^{hh}$, $\Delta L_{i,t}^{he}$ and $\Delta L_{i,t}^{qe}$ would all be useful to pattern 3. Consumers are willing to increase such energy demand at no cost, as the energy procurement cost would be reduced.

The incentive payment for IL $C_{i,t}^{IL}$ can be calculated according to (13).

$$C_{i,t}^{IL} = \alpha_i \Delta L_{i,t}^{ee2} + \beta_i \Delta L_{i,t}^{ee} \quad (13)$$

where α_i and β_i are coefficients varying with consumers.

The amount of IL should satisfy the upper and lower bound constraints.

$$\Delta L_{i,\min}^{ee} \le \Delta L_{i,t}^{ee} \le \Delta L_{i,\max}^{ee} \quad (14)$$

On the other hand, the increment of heating and cooling demand is affected by the incentive price, which can be estimated by the demand elasticity, as shown in (15).

$$\frac{\Delta L_i^h \cdot \lambda_h}{L_i^h \cdot \rho_h} = \varepsilon_i \quad (15)$$

Theoretically, the demand will reach its maximum value if the commodity becomes free, in other words, if the incentive price equals the energy price, as shown in (16).

$$\Delta L_i^h = L_{i,\max}^h - L_i^h, \quad if\ \rho_h = \lambda_h \quad (16)$$

Thus, we can obtain the elasticity of consumers with full compensation.

$$\varepsilon_i = \frac{L_{i,\max}^h - L_i^h}{L_i^h} \quad (17)$$

B. DEMAND-SUPPLY INTERACTION MODEL

CCHP usually works at heat-match mode, the power generation is bounded to the heat demand and cannot be changed flexibly. By encouraging the interaction between demand and supply, CCHP could serve as an efficient demand side resource.

Given a certain generation level or operation point, the relationship among the electricity output, heating output and cooling output of CCHP could be described as (18).

$$P_{j,t}^e = \left(P_{j,t}^h + P_{j,t}^q/\sigma_{hq}\right)/\sigma_{eh} \quad (18)$$

In practice, the heat-to-electricity ratio σ_{eh} is not a constant value, but varies with different generation levels [27], which can be illustrated by Fig.2. As a result, the increment of power generation, as can be expressed as (19), is not linear with that of heat.

$$\Delta P_{j,t}^e = \frac{P_{j,t}^h + \Delta P_{j,t}^h + \left(P_{j,t}^q + \Delta P_{j,t}^q\right)/\sigma_{hq}}{\sigma_{eh}} - P_{j,t}^e \quad (19)$$

where $\Delta P_{j,t}^h$ and $\Delta P_{j,t}^q$ are the increment of heating and cooling output, respectively.

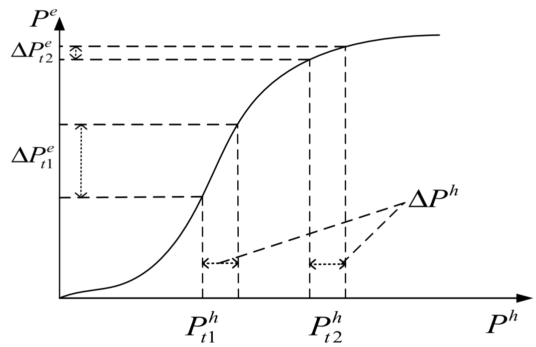

FIGURE 2. Heat-to-electricity ratio of CHP.

As can be seen from Fig.2, the incentive paid by the operator for cutting down the same amount of electric load at one moment is not equal to that at another moment. For example, when the heat output increases for the same amount ΔP^h, the increment of electricity output at t1is more than that at t2. Therefore, it is more economic to dispatch CCHP at t1 than at t2. Generally, as the generation level increases, both the response capacity and the economic benefits would drop. From the perspective of the operator, this interaction pattern would be applied in priority when such payment is cheaper than the payment for IL.

Nevertheless, due to the existence of multi-energy demand coupling, the load shaved by pattern 3 may be not equal to $\Delta P_{j,t}^e$. As mentioned before, if the value of μ_{eh} or μ_{eq} is positive, the electric load will increase with the heating and cooling loads and jeopardize the effect of pattern 3. To avoid this from happening, the following constraints should be satisfied.

$$\Delta P_{j,t}^e - \mu_{eh}\Delta L_{i,t}^{he} - \mu_{eq}\Delta L_{i,t}^{qe} \ge 0 \quad (20)$$

On the other side, the increment of heating and cooling generation is subject to that of corresponding demand, which has a limit. The thermal energy storage could help to relieve this restriction by storing the excessive heat temporally and releasing it in the subsequent periods. The operation of thermal energy storage can be described as follow.

$$S_{t+1}^{es} = S_t^{es}(1-\delta_{es}) + P_{in,t}^{es}\eta_{in} - \frac{P_{out,t}^{es}}{\eta_{out}} \quad (21)$$

$$0 \le P_{in,t}^{es} \le u_{es}P_{in,\max}^{es}, \quad u_{es}=0,1 \quad (22)$$

$$0 \le P_{out,t}^{es} \le (1-u_{es})\,P_{out,\max}^{es} \quad (23)$$

$$S_{\min}^{es} \le S_t^{es} \le S_{\max}^{es} \quad (24)$$

$$S_1^{es} = S_T^{es} \quad (25)$$

C. OPTIMIZATION MODEL OF IDR

The objective of the operator is to minimize the total incentive payment for IL, heating and cooling, which can be described as following.

$$\min C_{sum} = \sum_{i=1}^{n}\sum_{t=1}^{T}[C_{i,t}^{IL} + \rho_h\Delta L_{i,t}^{h} + \rho_q\Delta L_{i,t}^{q}] \quad (26)$$

In addition to the constraints presented by (10)-(25), the following constraints should also be satisfied.

1) LOAD CURTAILMENT INDEX CONSTRAINT

$$\sum_{i=1}^{n}(L_{i,t}^{e}+\Delta L_{i,t}^{e}) - \sum_{j=1}^{m}(P_{j,t}^{e}+\Delta P_{j,t}^{e}) \le L_t^{lim} \quad (27)$$

where L_t^{lim} is the maximum limit of electric load at time t. The net load of IES should not exceed this value.

2) UPPER AND LOWER BOUNDS OF HEATING AND COOLING DEMANDS

$$0 \le \Delta L_{i,t}^{h} \le L_{i,\max}^{h} - L_{i,t}^{h} \quad (28)$$

$$0 \le \Delta L_{i,t}^{q} \le L_{i,\max}^{q} - L_{i,t}^{q} \quad (29)$$

3) LOAD BALANCE CONSTRAINTS

$$P_t^e + \sum_{j=1}^{m}(P_{j,t}^{e}+\Delta P_{j,t}^{e}) = \sum_{i=1}^{n}(L_{i,t}^{e}+\Delta L_{i,t}^{e}) \quad (30)$$

$$\sum_{j=1}^{m}(P_{j,t}^{h}+\Delta P_{j,t}^{h}) = \sum_{i=1}^{n}(L_{i,t}^{h}+\Delta L_{i,t}^{h}) + P_t^{es} \quad (31)$$

$$\sum_{j=1}^{m}(P_{j,t}^{q}+\Delta P_{j,t}^{q}) = \sum_{i=1}^{n}(L_{i,t}^{q}+\Delta L_{i,t}^{q}) \quad (32)$$

4) CCHP OPERATION CONSTRAINTS

$$P_{j,\min}^{e} \le P_{j,t}^{e} + \Delta P_{j,t}^{e} \le P_{j,\max}^{e} \quad (33)$$

$$P_{j,\min}^{h} \le P_{j,t}^{h} + \Delta P_{j,t}^{h} \le P_{j,\max}^{h} \quad (34)$$

$$-R_{down}^{e} \le P_{j,t+1}^{e} - P_{j,t}^{e} \le R_{up}^{e} \quad (35)$$

$$-R_{down}^{h} \le P_{j,t+1}^{h} - P_{j,t}^{h} \le R_{up}^{h} \quad (36)$$

Equations (33) and (34) represent the electricity and heat output bounds of CCHP, and equations (35) and (36) represent the ramp rate constraints of electricity output and heat output.

5) HEATING NETWORK CONSTRAINTS

$$T_{in} = (T_s - T_a)\,e^{-hl/C_w m_i} + T_a \quad (37)$$

$$T_{out} = (T_r - T_a)\,e^{hl/C_w m_i} + T_a \quad (38)$$

$$L^h = m_i C_w (T_{in} - T_{out}) \quad (39)$$

In practice, $hl/C_w m_i$ is very small. According to the equivalent infinitesimal $\lim_{\mu\to 0} e^{\mu} = 1+\mu$, (37) and (38) can be approximately linearized as [28]:

$$T_{in}^{t} = \left(T_s - T_a^t\right)\left(1 - hl/C_w m_i^t\right) + T_a^t \quad (40)$$

$$T_{out}^{t} = \left(T_r - T_a^t\right)\left(1 + hl/C_w m_i^t\right) + T_a^t \quad (41)$$

On the other hand, the nonlinear characteristic of CCHP heat-to-electricity ratio can be approximated by piecewise linearization. In this way, the proposed model has been transformed to a mixed integer quadratic optimization problem, which is solved using Matlab with Yalmip and Gurobi.

IV. NUMERICAL ANALYSIS

A. TEST SYSTEM AND PARAMETERS

An industrial IES in south China with two CCHPs and eight large consumers is introduced as the test system to illustrate the technique proposed in this paper. The typical load curves of electricity, heating and cooling are shown in Fig. 3. The load limit L_t^{lim} is 40MW at all periods. The topology diagram of the district heating network is shown in Fig. 4.

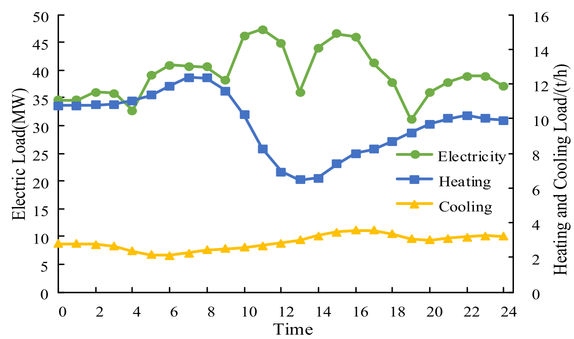

FIGURE 3. Typical load curves of electricity, heating and cooling.

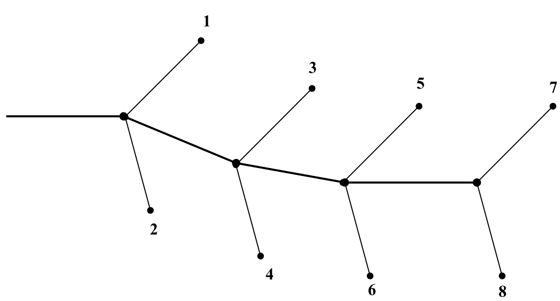

FIGURE 4. Topology diagram of the heating network.

The parameters of consumers' IL and coupling model are shown in Table 1 and Table 2, respectively. The coupling

TABLE 1. Parameters of IL.

Consumers	$\Delta L_{i,\max}^{ee}$ (MW)	$\Delta L_{i,\min}^{ee}$ (MW)	α	β
1	2	0	59	238
2	1.2	0	32	218
3	0.75	0	22	218
4	0.5	0	28	198
5	1.5	0	36	238
6	1	0	28	218
7	0.9	0	24	218
8	0.5	0	26	198

TABLE 2. Coupling coefficients of consumers.

Consumers	Proportion	μ_{eh}	μ_{eq}	μ_{hq}
1	20%	0.5	0	0.1
2	15%	0.5	1	0.1
3	10%	2	-1	0.1
4	5%	0	0.5	0.1
5	20%	0	-0.5	0.1
6	15%	-1	-0.5	0.1
7	10%	-2	1	0.1
8	5%	-0.5	0	0.1

coefficients are obtained through correlation analysis of consumers' energy data. The percentages of $L_{i,t}^{ee}$, $L_{i,t}^{eh}$ and $L_{i,t}^{eq}$ of all consumers are 50%, 30% and 20%, respectively. The percentages of $L_{i,t}^{hh}$, $L_{i,t}^{he}$ and $L_{i,t}^{hq}$ are 60%, 30% and 10%, respectively, and those of $L_{i,t}^{qq}$, $L_{i,t}^{qe}$ and $L_{i,t}^{qh}$ are 70%, 20% and 10%. The maximum heating demand and cooling demand are 14 tons and 4 tons, respectively.

The CCHP's output relationship between electricity and heat is demonstrated in Table 3, which is a piecewise linearization function. Other operation parameters of CCHP are shown in Table 4. The parameters of thermal energy storage are shown in Table 5. The parameters of the heating network are presented in Table 6.

TABLE 3. Generation characteristics of CCHP.

Electricity(MW)	Heat(t/h)	Electricity(MW)	Heat(t/h)
0	0	2.4	6.88
0.84	3.61	2.95	7.38
0.92	4.15	4.08	8.36
1.2	5.2	4.82	10
1.77	6.08		

TABLE 4. Parameters of CCHP.

$P_{j,\max}^{e}$ (MW)	$P_{j,\min}^{e}$ (MW)	$P_{j,\max}^{h}$ (t/h)	$P_{j,\min}^{h}$ (t/h)	R_{up}^{e} (MW)	R_{down}^{e} (MW)	R_{up}^{h} (t/h)	R_{down}^{h} (t/h)
4.82	0.84	10	3.61	2	2	4	4

The time-of-use electricity prices are presented in Table 7. The energy prices for heating and cooling are 63\$/ton and

TABLE 5. Parameters of thermal energy storage.

η_{in}	η_{out}	δ_{es}	$P_{in,\max}^{es}$ (t/h)	$S_{\max}^{es}$ (t)	$S_{\min}^{es}$ (t)
0.96	0.96	0.02	0.8	2	0.4

TABLE 6. Parameters of heating network.

C_w (J/Kg °C)	h(W/m°C)	l(m)	T_s (°C)	T_r (°C)	T_n (°C)
4200	0.25	300	85	60	10

TABLE 7. Time-of-use electricity prices.

Hours	14-17,19-22	8-14,17-19,22-24	0-8
Price($/MWh)	178	118	78

68$/ton, respectively. Besides, the incentive prices for heating and cooling are assumed to be equal to the energy prices.

B. SIMULATION RESULTS

By solving the optimization model, we can analyze the effect of the three interaction patterns on the total load reduction.

As can be seen from Fig. 5, the total load curtailment consists of five parts, i.e. IL, E-H load, E-Q load, E-H CCHP, and E-Q CCHP. The E-H load refers to the electricity-heat coupling load, which is curtailed by applying pattern 2, whereas E-H CCHP means that the load is curtailed by applying pattern 3. The meanings of E-Q load and E-Q CCHP are similar.

As is shown in Fig. 5(b), pattern 3, namely the interaction between demand and supply, contributes the most to the total load curtailment, and IL contributes the least. This implies that the incentive paid for encouraging consumers' heating and cooling demand is generally cheaper than that for IL.

There are ten hours when the electric load needs to be shaved, which are 6-7, 10-12, 14-17. At 6-8, the load is shaved all through load coupling and supply-demand interaction, whereas IL contributes none. At 10, given that the original heat generation level is relatively high, the heating and cooling output increment for increasing the same amount of electricity output becomes larger, according to the analysis with Fig.2. As a consequence, the incentive payment becomes relatively expensive and the load shaved by IL surpasses that by CCHP. From 11 to 12, due to the same reason, the IL curtailed by E-H CCHP decreases whereas that by E-H load increases.

The heating and cooling outputs of CCHPs before and after IDR dispatch are shown in Fig. 6. At 11 and 15, both the heating output and the cooling output reach its upper bound, meaning that the response capacity of pattern 2 and 3 is fully employed. Besides, as the original cooling demand increases gradually from 10 to 17, the space for increment becomes smaller, thus the load curtailed by E-Q CCHP

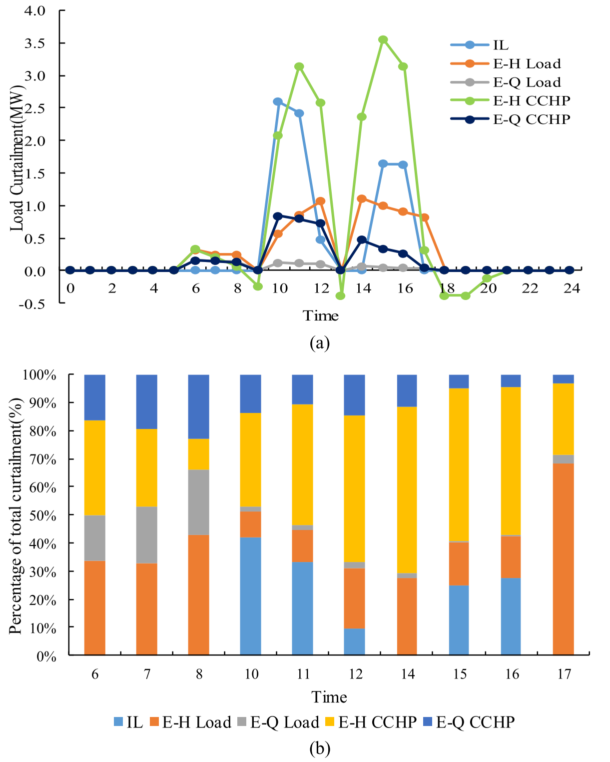

FIGURE 5. **Optimal dispatch plans. (a) Optimal dispatch plans of IL, E-H load, E-Q load, E-H CCHP and E-Q CCHP. (b) Percentage of each element to the total curtailment.**

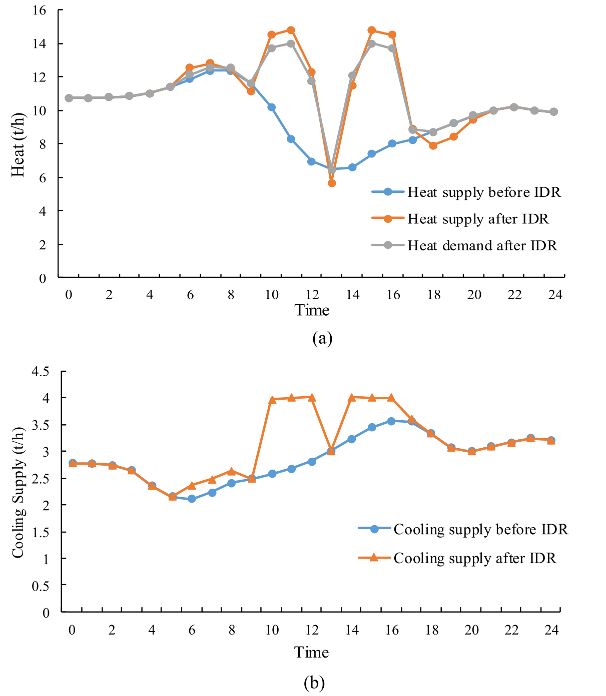

FIGURE 6. **Heating and cooling supply before and after IDR. (a) Heat supply before and after IDR. (b) Cooling supply before and after IDR.**

continues to drop. Due to the effect of thermal storage, the heat output could exceed the maximum value of demand. Moreover, the heat output of CCHP drops at 9, 13 and 18-20, as a result of energy storage releasing the heat stored previously.

Fig. 7 shows how consumers' demands for electricity, heating and cooling change during the interaction. Although pattern 2 is applied at every hour, the capacity of the coupling loads is limited. Therefore, when the amount of load that needs to be shaved is relatively large, such as at 10, 11, 15 and 17, the electric load is curtailed mostly by IL. Besides, at 10-16, the heating and cooling demands are mainly stimulated for increasing the output of CCHP, which contributes the most to the load curtailment.

Fig. 8(a) and (b) show how $\Delta L_{i,t}^{he}$ and $\Delta L_{i,t}^{qe}$ of each consumer changes during the interaction, respectively. It can be seen that only the heating demand of consumer 6, 7, 8, and the cooling demand of consumer 3, 5, 6 increase during the interaction, whereas the demand of others remains unchanged. Since the coupling coefficients of others are positive, the increase of these consumers' heating or cooling demands would have the counter effect and jeopardize the performance of pattern 3.

The load curves after IDR dispatch are demonstrated in Fig. 9. By applying the three interaction patterns, the load curtailment goal could be achieved, and the consumption for heating and cooling could be stimulated.

C. PROFITS ANALYSIS

To prove the economy of the mechanism proposed, two scenarios are simulated. In scenario I, the IDR mechanism with all the three pattern is applied, while in scenario II the conventional DR mechanism with only pattern 1 is applied. The dispatch cost paid by the operator, the profits gained by CCHP and the average energy procurement cost of consumers under these two scenarios are compared in Table 8.

TABLE 8. **Comparison of profits in scenario I and II.**

Scenario	Cost of operator($)	Revenue of CCHPs($)	Energy procurement cost of consumers ($/ton)
I	4461.08	4919.50	359.62
II	8399.31	0	406.85

As can be seen from the table, the total incentive payment in scenario I drops significantly by 46.9%, compared to that in scenario II. In practice, this value may vary with different energy prices, but the conclusion remains unchanged. In contrast with the conventional DR mechanism where there is only one pattern to achieve load curtailment, the operator is able to select interaction patterns of lower incentive payment, so the dispatch cost will inevitably decrease. The simulation results also show that if the coupling of energy demand is not taken in account, the dispatch cost will increase to $5996.82. Under this circumstance, both the amount of IL and the increment of heating or cooling loads will rise in order to fulfill the load curtailment constraint. Therefore, the compensation cost of the operator will also rise.

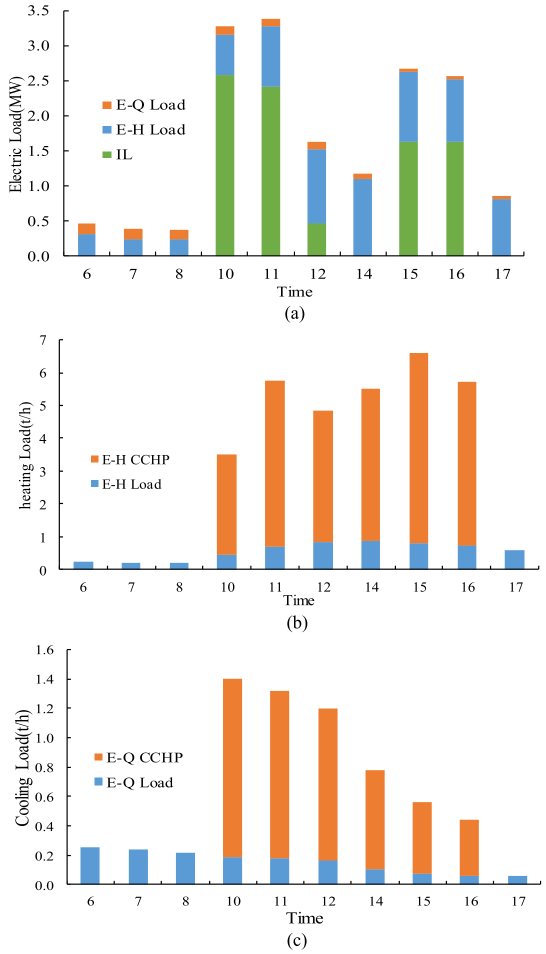

FIGURE 7. Change of electric, heating and cooling load. (a) Curtailment of consumers' electric load. (b) Increment of consumers' heat load. (c) Increment of consumers' cooling load.

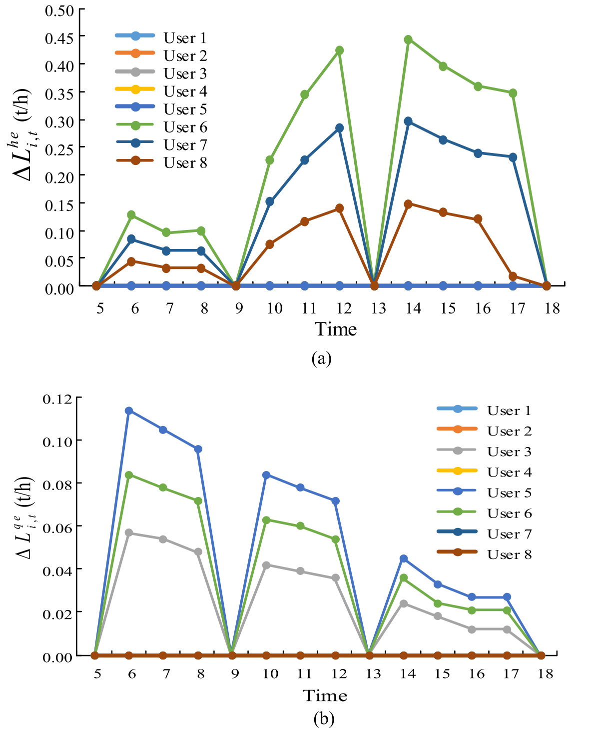

FIGURE 8. Heating and cooling loads increased by pattern 2. (a) Heating load increased by pattern 2. (b) Cooling load increased by pattern 2.

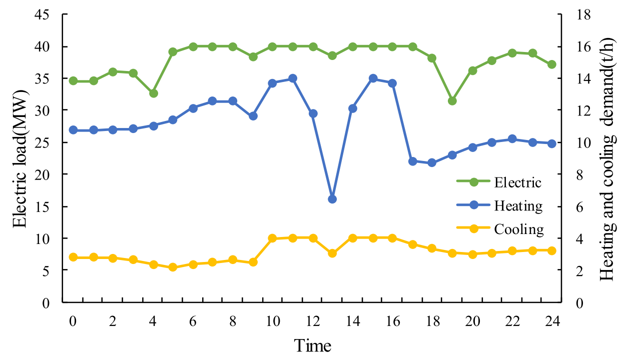

FIGURE 9. Load curves after IDR.

CCHP could also benefit from IDR. Its sales revenues on electricity, heating and cooling all increase, as pattern 2 and pattern 3 stimulate the energy demands of consumers. Furthermore, the consumers' average energy procurement cost for heating and cooling will also decrease, due to the compensation paid by the operator. In this sense, this mechanism could benefit all the participants and improve the social welfare.

D. IMPACT OF COUPLING CHARACTERISTICS

The effect of pattern 2 and 3 is largely dependent on consumers' multi-energy coupling characteristics. To analyze its impact on the optimal dispatch results, we set another two scenarios as comparison. In scenario III, μ_{eh} of all consumes is equal to 1 and μ_{eq} is equal to 0.5. In this way, the increase of their heating or cooling loads would also cause the increase of electric load. In contrast, the coupling coefficients in scenario IV are equal to those in scenario III, but the values are negative. The simulation results are shown in Fig. 10 and Fig. 11, respectively.

As can be seen from Fig. 10, due to the counter effect of positive coupling coefficients, pattern 2 is completely not implemented. As a consequence, the load curtailed through pattern 1 and 3 increases significantly, particularly through generating more cooling power. In scenario IV, the opposite results can be observed. Compared to scenario I, the load reduced by pattern 2 increases dramatically, accompanied by a sharp drop in IL. The contribution of pattern 3 also declines slightly.

The costs of each pattern in the three scenarios are presented in Table 9. In contrast with scenario I, the costs of pattern 1 and 3 all increase, especially the latter. As a result, the overall cost of scenario III is the highest, but still lower than that in scenario II. On the other hand, the costs of scenario IV is the lowest among the three scenarios. The expenses caused by pattern 1 and 3 are all lower than that of scenario I, whereas the cost of pattern 2 is apparently higher.

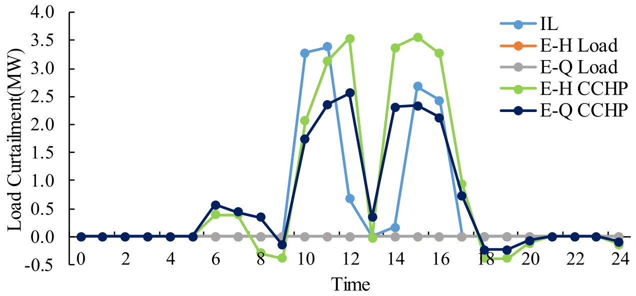

FIGURE 10. Optimal dispatch plan in scenario III.

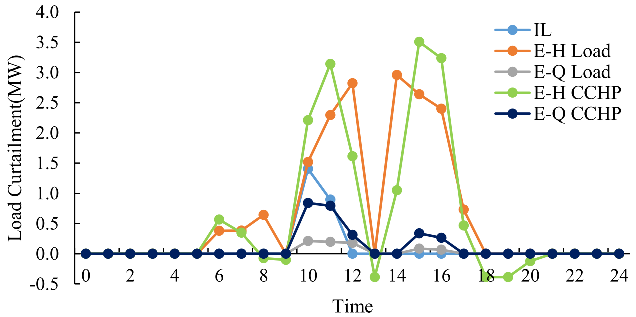

FIGURE 11. Optimal dispatch plan in scenario IV.

TABLE 9. Comparison of costs in scenario I, III and IV.

Scenarios	Cost of Pattern1($)	Cost of Pattern 2($)	Cost of Pattern 3($)	Overall Cost
I	1914.72	462.51	2083.84	4461.08
III	2820.25	0	3176.57	5996.82
IV	490.69	1166.24	1021.86	2678.79

This reflects the influence of multi-energy coupling coefficients on the optimal dispatch results. The negative coupling characteristics could effectively improve the performance of IDR and reduce the overall costs, whereas positive characteristics could only produce the counter effect.

E. IMPACT OF INCENTIVE PRICE

In the analysis above, the incentive prices are assumed to be equal to corresponding energy prices, which could motivate consumers as much as possible. However, paying consumers with full compensation may not be the best option for the operator. Thus, we simulate how the total incentive payment changes with different incentive prices, and the results are shown in Fig. 12.

Apparently, as the incentive price increases, the total cost gradually drops at first, and then rises after reaching the minimum point, which is mainly attributed to the demand elasticity and the output characteristics of CCHP. In this case, the optimal incentive price adopted by the operator should be 75% of the corresponding energy price. This founding helps the operator to determine the best incentive price so as to minimize the dispatch cost and optimize the allocation of resources.

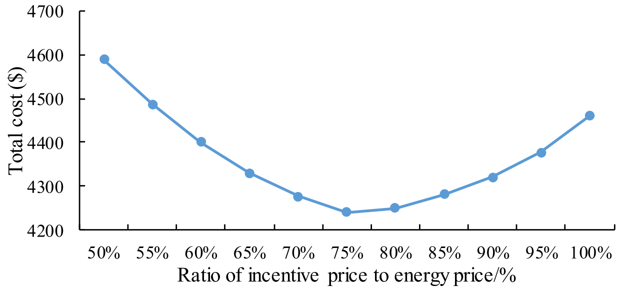

FIGURE 12. Impact of incentive price on the total cost.

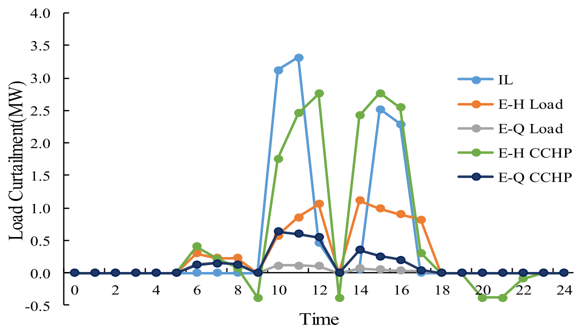

FIGURE 13. Optimal dispatch plans under the best incentive price.

The load curtailment under the best incentive price is shown in Fig. 13. Compared to Fig. 5(a), the amount of IL increases, whereas the amount of E-H CCHP and E-Q CCHP drops as a consequence of lower incentive level.

V. CONCLUSION

By incorporating consumers' heating and cooling demand into the dispatch of IDR, this paper proposes an IDR mechanism with three effective incentive patterns for load curtailment. The incentive is paid for increasing heating and cooling loads, which could improve consumers' motivation. Based on the coupling model of multi-energy demand and the demand-supply interaction model, the optimization model of IDR is established with the objective of minimizing the total dispatch cost. Simulation results prove that the mechanism proposed could effectively achieve the load curtailment through multi-energy interaction. Compared to conventional DR programs, the total dispatch cost of the operator and the energy procurement cost of consumers are both reduced. CCHP could also gain reasonable revenue. Therefore, the total social welfare has increased. The effect of increasing the electricity output of CCHP by stimulating heat loads may be jeopardized due to the coupling of multi-energy demand. Furthermore, we also analyze how the value of incentive price affects the dispatch cost, which is crucial for the determination of incentive price. Importantly, the dispatch model proposed in this paper could be applied not only to the curtailment of electric load but also to that of heating or cooling loads.

REFERENCES

[1] Z. Zhou, F. Zhao, and J. Wang, "Agent-based electricity market simulation with demand response from commercial buildings," *IEEE Trans. Smart Grid*, vol. 2, no. 4, pp. 580–588, Dec. 2011.

[2] F. Rahimi and A. Ipakchi, "Demand response as a market resource under the smart grid paradigm," *IEEE Trans. Smart Grid*, vol. 1, no. 1, pp. 82–88, Jun. 2010.

[3] J. Wang, H. Zhong, Z. Ma, Q. Xia, and C. Kang, "Review and prospect of integrated demand response in the multi-energy system," *Appl. Energy*, vol. 202, pp. 772–782, Sep. 2017.

[4] M. Qadrdan, M. Cheng, J. Wu, and N. Jenkins, "Benefits of demand-side response in combined gas and electricity networks," *Appl. Energy*, vol. 192, pp. 360–369, Apr. 2017.

[5] S. M. Nosratabadi, R.-A. Hooshmand, and E. Gholipour, "Stochastic profit-based scheduling of industrial virtual power plant using the best demand response strategy," *Appl. Energy*, vol. 164, pp. 590–606, Feb. 2016.

[6] Z. Xu, Z. Hu, Y. Song, and J. Wang, "Risk-averse optimal bidding strategy for demand-side resource aggregators in day-ahead electricity markets under uncertainty," *IEEE Trans. Smart Grid*, vol. 8, no. 1, pp. 96–105, Jan. 2017.

[7] Z. Li, W. Wu, and B. Zhang, "Coordinated state-estimation method for air-conditioning loads to provide primary frequency regulation service," *IET Gener., Transmiss. Distrib.*, vol. 11, no. 13, pp. 3381–3388, Sep. 2017.

[8] G. Benysek, J. Bojarski, R. Smolenski, M. Jarnut, and S. Werminski, "Application of stochastic decentralized active demand response (DADR) system for load frequency control," *IEEE Trans. Smart Grid*, vol. 9, no. 2, pp. 1055–1062, Mar. 2018.

[9] W. Liu, Q. Wu, F. Wen, and J. Østergaard, "Day-ahead congestion management in distribution systems through household demand response and distribution congestion prices," *IEEE Trans. Smart Grid*, vol. 5, no. 6, pp. 2739–2747, Nov. 2014.

[10] J. Wu, B. Zhang, and Y. Jiang, "Optimal day-ahead demand response contract for congestion management in the deregulated power market considering wind power," *IET Gener., Transmiss. Distrib.*, vol. 12, no. 4, pp. 917–926, Feb. 2018.

[11] S. Bahrami and A. Sheikhi, "From demand response in smart grid toward integrated demand response in smart energy hub," *IEEE Trans. Smart Grid*, vol. 7, no. 2, pp. 650–658, Mar. 2016.

[12] Z. Liang, Q. Alsafasfeh, T. Jin, H. Pourbabak, and W. Su, "Risk-constrained optimal energy management for virtual power plants considering correlated demand response," *IEEE Trans. Smart Grid*, vol. 10, no. 2, pp. 1577–1587, Mar. 2019.

[13] C. Zhang, Y. Xu, Z. Li, and Z. Y. Dong, "Robustly coordinated operation of a multi-energy microgrid with flexible electric and thermal loads," *IEEE Trans. Smart Grid*, vol. 10, no. 3, pp. 2765–2775, May 2019.

[14] H. Cui, F. Li, Q. Hu, L. Bai, and X. Fang, "Day-ahead coordinated operation of utility-scale electricity and natural gas networks considering demand response based virtual power plants," *Appl. Energy*, vol. 176, pp. 183–195, Aug. 2016.

[15] M. Pau, J. L. Cremer, F. Ponci, and A. Monti, "Impact of customers flexibility in heat pumps scheduling for demand side management," in *Proc. IEEE Int. Conf. Environ. Elect. Eng., IEEE Ind. Commercial Power Syst. Eur.*, Milan, Italy, Jun. 2017, pp. 1–6.

[16] G. Papaefthymiou, B. Hasche, and C. Nabe, "Potential of heat pumps for demand side management and wind power integration in the German electricity market," *IEEE Trans. Sustain. Energy*, vol. 3, no. 4, pp. 636–642, Oct. 2012.

[17] N. Good, E. Karangelos, A. Navarro-Espinosa, and P. Mancarella, "Optimization under uncertainty of thermal storage-based flexible demand response with quantification of residential users' discomfort," *IEEE Trans. Smart Grid*, vol. 6, no. 5, pp. 2333–2342, Sep. 2015.

[18] M. Tasdighi, H. Ghasemi, and A. Rahimi-Kian, "Residential microgrid scheduling based on smart meters data and temperature dependent thermal load modeling," *IEEE Trans. Smart Grid*, vol. 5, no. 1, pp. 349–357, Jan. 2014.

[19] Y. Kim and L. K. Norford, "Optimal use of thermal energy storage resources in commercial buildings through price-based demand response considering distribution network operation," *Appl. Energy*, vol. 193, pp. 308–324, May 2017.

[20] A. Arteconi, D. Patteeuw, K. Bruninx, E. Delarue, W. D'haeseleer, and L. Helsen, "Active demand response with electric heating systems: Impact of market penetration," *Appl. Energy*, vol. 177, pp. 636–648, Sep. 2016.

[21] N. Liu, J. Wang, L. Ma, and X. Yu, "Hybrid energy sharing for smart building cluster with CHP system and PV prosumers: A coalitional game approach," *IEEE Access*, vol. 6, pp. 34098–34108, 2018.

[22] N. Liu, L. He, X. Yu, and L. Ma, "Multiparty energy management for grid-connected microgrids with heat- and electricity-coupled demand response," *IEEE Trans. Ind. Informat.*, vol. 14, no. 5, pp. 1887–1897, May 2018.

[23] C. Shao, Y. Ding, J. Wang, and Y. Song, "Modeling and integration of flexible demand in heat and electricity integrated energy system," *IEEE Trans. Sustain. Energy*, vol. 9, no. 1, pp. 361–370, Jan. 2018.

[24] S. Chen, Z. Wei, G. Sun, K. W. Cheung, and D. Wang, "Identifying optimal energy flow solvability in electricity-gas integrated energy systems," *IEEE Trans. Sustain. Energy*, vol. 8, no. 2, pp. 846–854, Apr. 2017.

[25] M. Geidl, G. Koeppel, P. Favre-Perrod, B. Klockl, G. Andersson, and K. Frohlich, "Energy hubs for the future," *IEEE Power Energy Mag.*, vol. 5, no. 1, pp. 24–30, Jan./Feb. 2007.

[26] A. Gholian, H. Mohsenian-Rad, and Y. Hua, "Optimal industrial load control in smart grid," *IEEE Trans. Smart Grid*, vol. 7, no. 5, pp. 2305–2316, Sep. 2016.

[27] C. Wu, P. Jiang, W. Gu, and Y. Sun, "Day-ahead optimal dispatch with CHP and wind turbines based on room temperature control," in *Proc. IEEE Int. Conf. Power Syst. Technol.*, Sep./Oct. 2016, pp. 1–6.

[28] X. S. Jiang, Z. X. Jing, Y. Z. Li, Q. H. Wu, and W. H. Tang, "Modelling and operation optimization of an integrated energy based direct district water-heating system," *Energy*, vol. 64, no. 1, pp. 375–388, Jan. 2014.

ZIQING JIANG (S'17) received the B.S. degree in electrical engineering from Southeast University, Nanjing, China, in 2016. He is currently pursuing the Ph.D. degree in electrical engineering with Shanghai Jiao Tong University, Shanghai, China. His research interests include demand response, electricity market, and regional integrated energy systems.

QIAN AI (M'03–SM'16) received the B.S. degree from Shanghai Jiao Tong University, Shanghai, China, in 1991, the M.S. degree from Wuhan University, Wuhan, China, in 1994, and the Ph.D. degree from Tsinghua University, Beijing, China, in 1997, all in electrical engineering. He was with Nanyang Technological University, Singapore, for one year, and also with the University of Bath, U.K., for two years. He is currently a Professor with the Department of Electrical Engineering, Shanghai Jiao Tong University. His research interests include load modeling, smart grid, microgrids, virtual power plant, regional integrated energy systems, big data, and artificial intelligence.

RAN HAO (S'17) received the B.S. degree in electrical engineering from Xi'an Jiaotong University, Xi'an, China, in 2016. He is currently pursuing the Ph.D. degree in electrical engineering with Shanghai Jiao Tong University, Shanghai, China. His research interests include the energy internet and microgrid.